Nuclear Instruments and Methods in Physics Research A 678 (2012) 91–97

Contents lists available at SciVerse ScienceDirect

Nuclear Instruments and Methods in Physics Research A

journal homepage: www.elsevier.com/locate/nima

Spin filtering neutrons with a proton target dynamically polarized using photo-excited triplet states

M. Haag [a], B. van den Brandt [a], T.R. Eichhorn [a,b], P. Hautle [a,*], W.Th. Wenckebach [a,1]

[a] Paul Scherrer Institute, CH-5232 Villigen PSI, Switzerland
[b] Laboratory for Functional and Metabolic Imaging, Ecole Polytechnique Fédérale de Lausanne, CH-1015 Lausanne, Switzerland

ARTICLE INFO

Article history:
Received 12 December 2011
Received in revised form
24 February 2012
Accepted 4 March 2012
Available online 22 March 2012

Keywords:
Neutron polarization analysis
Spin filters
Dynamic nuclear polarization
Photo-excited triplet states

ABSTRACT

In a test of principle a neutron spin filter has been built, which is based on dynamic nuclear polarization (DNP) using photo-excited triplet states. This DNP method has advantages over classical concepts as the requirements for cryogenic equipment and magnets are much relaxed: the spin filter is operated in a field of 0.3 T at a temperature of about 100 K and has performed reliably over periods of several weeks.

The neutron beam was also used to analyze the polarization of the target employed as a spin filter. We obtained an independent measurement of the proton spin polarization of ~ 0.13 in good agreement with the value determined with NMR. Moreover, the neutron beam was used to measure the proton spin polarization as a function of position in the naphthalene sample. The polarization was found to be homogeneous, even at low laser power, in contradiction to existing models describing the photo-excitation process.

1. Introduction

Dynamic nuclear polarization (DNP) [1] has not only lead to the development of increasingly sophisticated polarized targets with which the role of spin in nuclear and particle interactions is investigated, but they have also opened new possibilities in neutron science by exploiting the strong spin dependence of the neutron scattering on protons [2–4]. Proton polarization values close to unity have been achieved in some cases with the classical method of DNP, applied to solid samples that contain spatially immobile electron spins in addition to the nuclear spins of interest. However, they have the clear disadvantage that they require temperatures of 1 K or lower and fields of several tesla. This drawback can be relieved with a more recent and very promising DNP method that uses short-lived photo-excited triplet states and requires neither low temperatures nor high fields [5]. This is immediately attractive in view of applications as technically simpler systems with open geometries become feasible. In this paper we present a proof of principle of a spin filter for slow neutrons, which is based on this technique.

2. Neutron polarization devices

Super mirror polarizers are the standard device for neutron beam polarization and the analysis of scattered neutrons [6]. They rely on spin-dependent neutron optical reflection. They are easy to set up and use, have a high polarizing efficiency for cold and thermal neutrons, are stable in time and need no maintenance. However, these instruments are restricted in their angular acceptance and the neutron energy is limited to energies below 20 meV (corresponding to wavelengths longer than 2 Å).

These limitations do not exist for neutron spin filters. They rely on spin-dependent nuclear scattering, e.g., on polarized protons [7], or absorption on polarized ^{3}He [8]. The analyzing power and transmission of a homogeneous spin filter with parallel entrance and exit windows perpendicular to the beam are practically independent on the beam divergence. This leads to a principle advantage for high precision neutron polarimetry [9,10]. More importantly, spin filters can polarize the whole range of cold, thermal and hot neutrons. With the advent of strong pulsed neutron spallation sources this property becomes crucial, since they allow time-of-flight methods to be employed to analyze all wavelengths in a single experiment [11].

Spin filters of optically polarized ^{3}He have been developed and are available at several neutron research centers and present efforts [12] aim to further optimize this technique. However, the strong energy dependence of the absorption cross-section makes it difficult to optimize the filter thickness for a large neutron energy range.

Broadband spin filters using dynamically polarized protons offer an attractive alternative, as was realized and demonstrated already long ago [7]. Such a polarized proton spin filter is based on the strong dependence of the neutron–proton scattering on the relative orientation of their spins. The resulting spin-dependent cross-section is usefully large up to the sub-MeV region. However,

* Corresponding author. Tel.: +41 56 310 3210.
E-mail address: patrick.hautle@psi.ch (P. Hautle).
[1] Academic guest.

0168-9002/$ - see front matter © 2012 Elsevier B.V. All rights reserved.
http://dx.doi.org/10.1016/j.nima.2012.03.014

an actual implementation of a polarized proton spin filter has been so far restricted to a few special cases, e.g., for a precise beam polarization determination [14] or to polarize neutrons of thermal [15] and epithermal energy where it is the only method currently available [16].

In neutron spin filters based on dynamic nuclear polarization (DNP) one polarizes electron spins by cooling them down to low temperature and applying a strong magnetic field. Next one transfers the high polarization of electron spins to the nuclear spins by means of a microwave field. Unfortunately, the cryogenic equipment and the superconducting magnet needed for this purpose strongly limit access to the filter, thus reducing its potential for application.

On the other hand, in DNP using optically excited triplet states, the triplet electron spin is polarized as a result of the optical selection rules. Then the requirements for the cryogenic equipment and the magnetic field are significantly relaxed making technically simpler systems possible. A first exploratory experiment was performed by Ref. [17]. Here we present a proof of principle that a neutron spin filter based on this method can be built.

Below we first discuss the principles of a polarized proton spin filter and present a short outline of the method of DNP using photo-excited triplet states. Next, we shortly describe the experimental methods and present the performance of the spin filter. We furthermore use the spin filter to perform an independent determination of the proton spin polarization and to show that it is homogeneous in the filter. The latter is not only important for the operation of the spin filter, but also of interest for the understanding of the mechanism of DNP using this method.

3. Neutron spin filtering with polarized protons

The working principle of a polarized proton spin filter is based on the fact that the singlet cross-section for neutron–proton scattering is much higher than the triplet cross-section [18–20]. This is the case for coherent and incoherent scattering. Hence, neutrons polarized anti-parallel to the protons will thus be much stronger scattered than those polarized parallel. As a result the polarization of the neutron beam changes while it passes through the spin filter material. It is customary to define a spin-dependent effective cross-section

$$\sigma_{\pm} = \sigma_0 \pm \sigma_p P \tag{1}$$

where the $+$ and the $-$ stand for the two eigenstates of the neutron spin with respect to the target's polarization axis. The spin-dependent part is the product of the 'polarization cross-section' σ_p and the nuclear polarization P. The term σ_0 denotes the neutron spin-independent cross-section.

After passing through the spin filter with a proton density N and a thickness d, the two spin components of the neutron beam are attenuated by a factor $\exp(-\sigma_{\pm} Nd)$. Thus, an initially unpolarized neutron beam will have a polarization behind the filter of

$$A = \tanh(\sigma_p PNd) \tag{2}$$

which is called the filter analyzing power. The thicker the filter, the higher the filter analyzing power for given $(\sigma_p N)$, and the lower the transmission T of the neutron beam

$$T = \exp(-\sigma_0 Nd)\cosh(\sigma_p PNd). \tag{3}$$

Remark that for a given analyzing power A, the total transmission T increases with the filter polarization P.

The polarization cross-section σ_p for a specific material is normally determined experimentally as structural effects observed for slow neutrons can only be treated well theoretically if the sample structure is sufficiently well known. Fig. 1 gives the general trend for the value of σ_p as a function of the incoming neutron energy. It is qualitatively correct for most hydrogenous materials. For long wavelengths above about 5 Å, the cross-section is determined by incoherent scattering and absorption on bound nuclei. With decreasing wavelength the neutrons start to resolve the chemical structure of the sample, giving rise to coherent scattering, most prominent between 2 and 5 Å. For even shorter wavelengths inelastic scattering starts to have an effect and the cross-section approaches for energies larger than inter-atomic bonds ($E > 1$ eV) the one given by the scattering of isolated free protons [21].

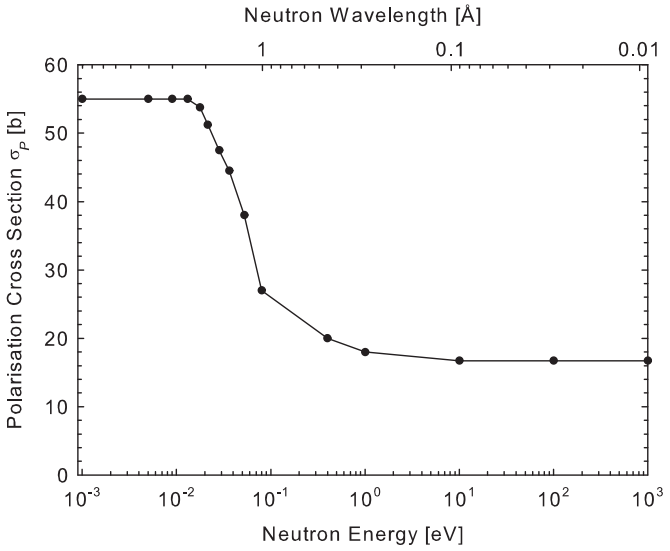

Fig. 1. Typical trend of the polarization cross-section σ_p as function of the neutron wavelength, respectively, neutron energy. The data points are a compilation of literature values [7,15,16,22].

4. Polarizing protons via photo-excited triplet states

The gist of DNP is to exploit the high polarization of an electron spin system by transferring it to the nuclear spin system with a microwave field. In the classical schemes the unpaired electrons of paramagnetic dopants are used and their spin polarization is determined thermally. This requires cooling the sample to temperatures of about 1 K or below and applying a magnetic field of several tesla.

An attractive alternative is the use of photo-excited triplet states instead of ground state paramagnetic dopants. The polarization of the triplet electron spin is determined by the photo-excitation process and is often high and independent of temperature and magnetic field.

A proven system for triplet DNP is a naphthalene molecular host crystal doped with a small concentration of pentacene guest molecules. The latter can be optically excited into a triplet state where the triplet electron spin is strongly aligned. The excitation scheme is shown in Fig. 2. Using a short optical pulse the molecule is excited from the singlet ground state S_0 to the lowest excited singlet state S_1. From there the system either decays back to ground state, or decays via intersystem crossing (ISC) to the lowest triplet state T_1. While the life time of the lowest excited singlet state S_1 is only about 20 ns, the life time of the lowest triplet state T_1 is of the order 50 μs, allowing its use for DNP. The triplet spin levels are split by fine coupling and can be further split with an externally applied magnetic field, typically oriented along the X-axis of the pentacene molecule (see Fig. 3). With $B \| X$ two ESR lines are observed at ~ 0.3 T – separated by about

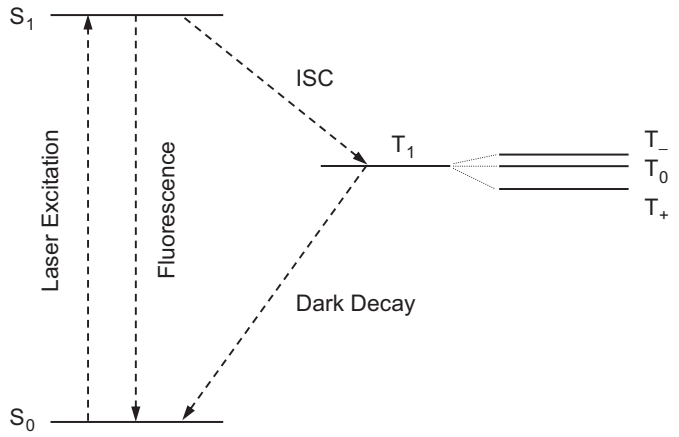

Fig. 2. A simplified energy level scheme of the pentacene molecule, showing the photo-physical processes during illumination with laser light. The triplet spin levels are split by fine coupling and can be further split with an externally applied magnetic field, typically oriented along the *X*-axis of the pentacene molecule giving levels denoted as T_-, T_0 and T_+.

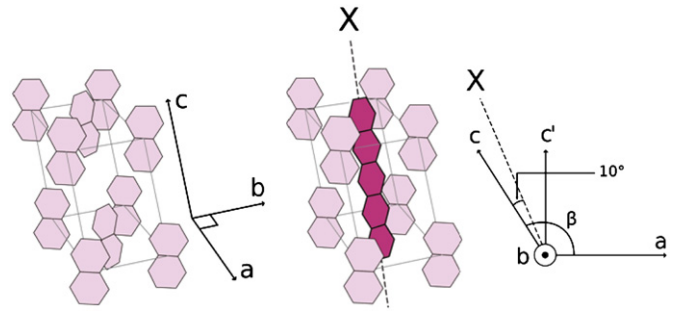

Fig. 3. Left: Unit cell of pure naphthalene whose crystal structure is monoclinic with axes $a \sim 8.2$ Å, $b \sim 6.0$ Å, $c \sim 8.7$ Å and $\beta = 123°$. The a–b plane is the cleavage plane. Right: Two naphthalene molecules can be replaced by one pentacene molecule whose *X*-axis lies in the a–c plane at an angle of 10° to the c-axis.

1.5 GHz – corresponding to the transitions −1 to 0 and 0 to 1 (see Fig. 2). In triplet DNP only one of the two ESR transitions is used and the two energy levels involved may be regarded as a highly polarized effective spin-$\frac{1}{2}$ system. For $B \| X$ the selection rules for the ISC process strongly favor the occupation of the triplet level T_0 resulting in a high "effective" electron spin polarization of ~ 0.9 [23]. Furthermore the electron spin lattice relaxation time is longer than the life time of the triplet state. Hence, the triplet electron spin polarization is not only independent of temperature and strength of the applied field, but also almost completely maintained during the life time of the triplet state.

The Integrated Solid Effect (ISE) scheme is proven to be the most efficient method to transfer the triplet electron polarization to the nuclear spins [5]. In this method the externally applied magnetic field is adiabatically swept over the inhomogeneously broadened ESR line (typically in 15 μs) under microwave irradiation, which allows all electron spin packets to constructively participate in the polarization transfer. For more details we refer to the founding paper [24]. As in classical DNP, the nuclear spin polarization thus created is localized around the triplet guest molecules but spreads out further over the host molecules via spin diffusion. By repeating the cycle many times the proton spin polarization is accumulated and approaches the maximum value given by the electron polarization. In naphthalene the proton spin lattice relaxation time is very long (~ 24 h at liquid nitrogen temperature). So DNP experiments need moderate cryogenic means only. High proton polarizations have been reached in fields on only 0.3 T at temperatures of 105 and 300 K [5,25]. Recently triplet DNP has been successfully implemented in a polarized target system for the use on radioactive ion beams [26].

5. Spin filter apparatus

The spin filter apparatus consists of the following main components: a helium flow cryostat cooling the sample to around 100 K, a small electro-magnet producing the static magnetic field of 0.3 T, a laser system that excites the triplet states, a combined pulse ESR/DNP system to observe the triplet states and to transfer their electron polarization to the protons, and a pulse NMR system to monitor the proton polarization. The whole system is controlled with home made software running under Labview. A detailed description of the apparatus will be given elsewhere.

5.1. Spin filter crystal

Large high quality naphthalene single crystals doped with pentacene were grown with a self-seeding vertical Bridgeman technique [27]. Pentacene deteriorates under light irradiation when exposed to oxygen. Therefore, the transfer of the zone refined naphthalene into the growth ampoule and the introduction of the pentacene was performed under a nitrogen atmosphere. The sample used in the neutron experiments is a rhomboid of $4.65 \times 5.6 \times 5.35$ mm^3 cut out of a several cm^3 single crystal. The pentacene concentration was determined with optical transmission spectroscopy to be $2.0 \pm 0.1 \times 10^{-5}$ mol/mol. The orientation of the crystal a, b and c-axes with respect to the x, y and z-axes of the rhomboid is shown in Fig. 4. The sample is cut such that its bottom (x–y-plane) corresponds to the crystal a–c-plane with its x-axis parallel to the pentacene molecular *X*-axis. The sample can be rotated about its vertical z-axis – corresponding to the crystal b-axis – in order to precisely align the pentacene *X*-axis with the horizontally applied magnetic holding field. The misalignment due to improper cutting and mounting is estimated from the shape of the ESR line to be less than 3°. The laser beam irradiates the sample from below along the crystal b-axis and the neutron beam traverses the 5.6 mm thick sample along the y-axis.

5.2. Procedure for DNP

To photo-excite the pentacene molecules into the triplet state we use a tripled Nd:YAG laser followed by an optical parametric

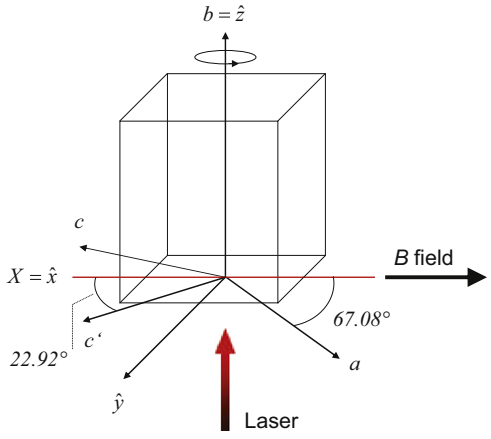

Fig. 4. Orientation of the sample mounted in the target system. The sample is cut such that the crystal b-axis coincides with the vertical z-axis and the laser beam direction. The pentacene molecular *X*-axis is parallel to the holding field and the neutron beam is along the y-axis.

oscillator tuned to 602 nm corresponding to the zero phonon $S_0 \rightarrow S_1$ transition. This laser system delivers 10 ns pulses with a repetition rate of 30 Hz and an energy of approximately 9.6 mJ per pulse at the entrance window of the cryostat. To polarize the proton spins ISE passages are performed, sweeping the magnetic field with 0.3 mT/μs and a microwave field corresponding to a Rabi frequency of the order of 5 MHz. Under these conditions a maximum polarization of around 13% is reached with a build up time constant of 5 h. Most measurements are performed with the proton polarization at this maximum, while keeping the DNP process going in order to prevent the polarization from slowly relaxing during the period (several hours) that neutron data are taken.

6. Neutron measurements—performance of the spin filter

6.1. Experimental procedure

The neutron spin filter experiment was performed at the new BOA beam line, an upgrade of the former FUNSPIN beam [13] at the continuous spallation neutron source SINQ at the Paul Scherrer Institute in Switzerland. A diagram of the experimental setup is given in Fig. 5. The incoming beam is polarized by the original bender and its spectral distribution is determined by the liquid deuterium moderator. With an adiabatic spin flipper [14] the neutron polarization can be reversed with respect to the polarity of the guide field at the polarized target. Its efficiency is $f = 0.98 \pm 0.005$. The neutron spin polarization is maintained throughout the beam path to the ^{3}He neutron detector with iron sheets magnetized with small permanent magnets. Diaphragms collimate the beam to about 2.5 mrad (FWHM) at the position of the target sample. A beam defining aperture of $3 \times 4\ \mathrm{mm}^2$ is located 15 mm before the target sample and fixed to the cryostat insert. The sample is aligned to the diaphragms by taking neutron radiography pictures with a CCD camera at the detector position. To perform measurements as a function of the neutron wavelength a chopper is placed before the spin flipper and the time of flight (TOF) is determined over the distance of about 7 m to the ^{3}He neutron detector.

6.2. Determination of the analyzing power

The analyzing power A of the polarized proton target is determined by comparing the count rate N_0 with spin flipper inactive to the count rate N_1 with spin flipper active and extracting it from the so-called flipping ratio [28]

$$R_F = \frac{N_0}{N_1} = \frac{1+pA}{1-fpA} \tag{4}$$

where p is the polarization of the neutron beam and f the efficiency of the spin flipper. The target polarization was negative throughout the experiment resulting in a negative analyzing power A. With the flipper active, neutron and proton polarization are parallel and the transmission through the filter is high. As all quantities depend on the neutron wavelength, R_F is measured with the TOF method. Fig. 6 shows typical spectra obtained for the two states of the spin flipper. Several TOF spectra were measured, each taking several hours per flipper state. In each run the proton polarization is continuously monitored by NMR and additionally a precise flipping ratio is measured with a white beam before and after each TOF run. Between the different runs the target polarization P varied between -0.12 and -0.13.

The wavelength dependence of the beam polarization $p(\lambda)$ is determined in a separate measurement where the polarized sample is lifted above the beam and a calibrated wide angle super mirror analyzer is used instead. The analyzer efficiency $A_{sm}(\lambda)$ is known to a precision of ± 0.005. The beam polarization determined with the known flipper efficiency f and Eq. (4) is shown in Fig. 7. Finally, using the thus obtained beam polarization, the known flipper efficiency f and the TOF spectra, the filter analyzing power is obtained using Eq. (4). The result is shown in

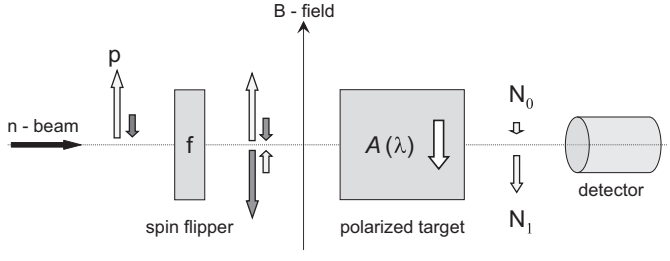

Fig. 5. Schematic side view of the spin filter setup. Remark that the spin filter polarization is negative and a high count rate (N_1) is obtained with the spin flipper active.

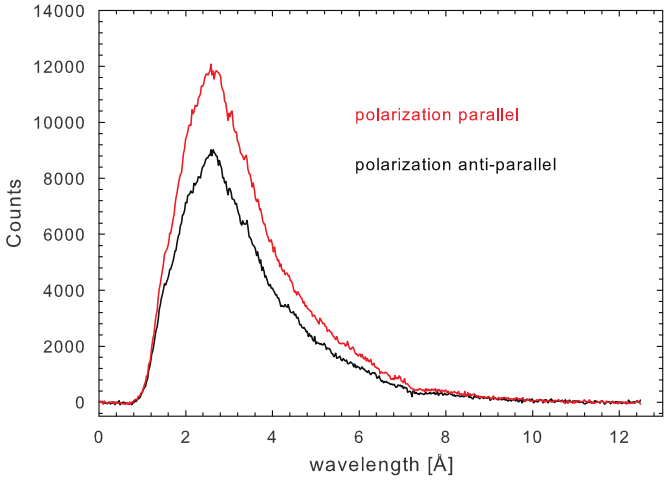

Fig. 6. Set of time of flight spectra measured for neutron spin parallel and anti-parallel to the target proton polarization which was $P \sim -0.13$.

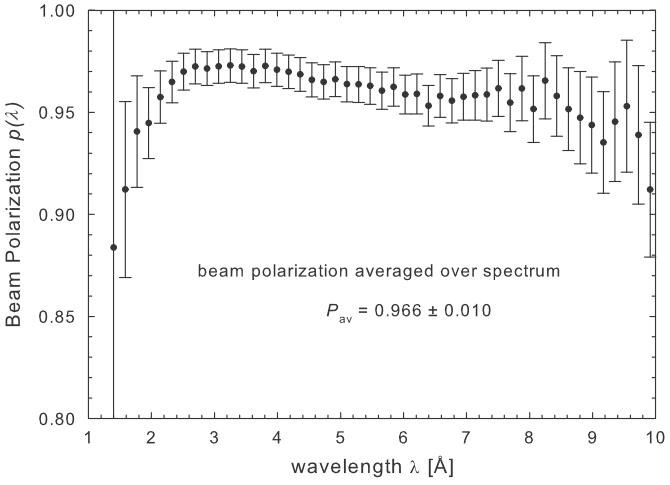

Fig. 7. Polarization of the neutron beam $p(\lambda)$ at the beam line BOA at SINQ measured with a wide angle super mirror analyzer. The error bar given is dominated by the uncertainties of f and $A_{sm}(\lambda)$. The beam polarization averaged over the wavelength spectrum is $\overline{p} = 0.966 \pm 0.010$.

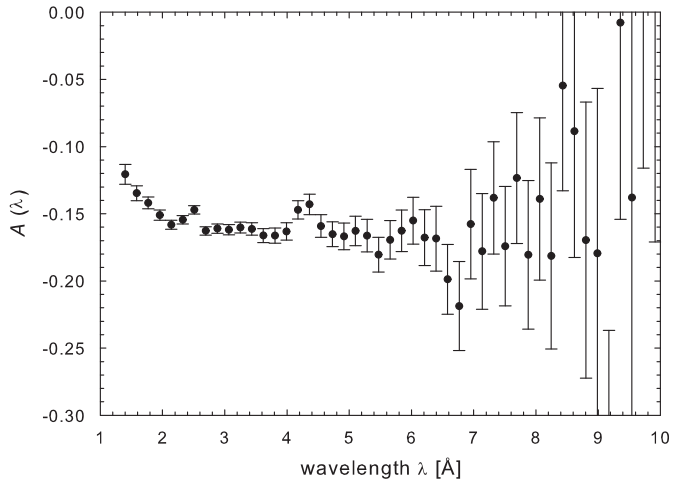

Fig. 8. Filter analyzing power $A(\lambda)$ of the polarized proton target with $P\sim-0.13$ as obtained from the spectra given in Fig. 6. The sources of errors are the counting statistics with the background correction and the errors of f and $p(\lambda)$.

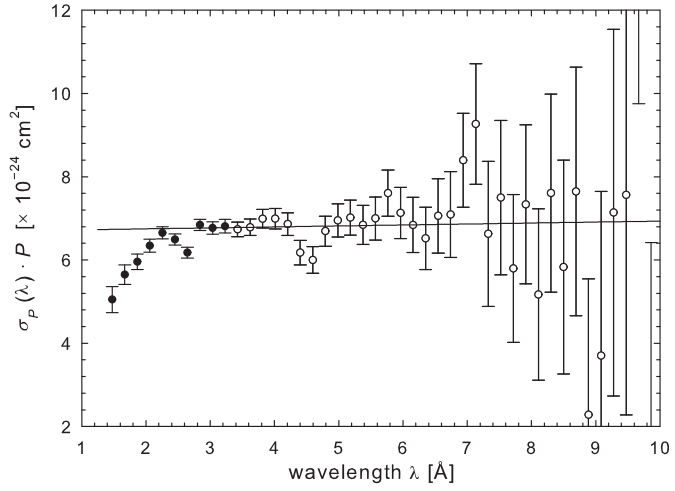

Fig. 9. Product of the polarization cross-section times the filter polarization determined via Eq. (5). The line is a fit of Eq. (6) to the data in the range of 3.3–9.5 Å and indicated by open circles. From this fit the average proton polarization P is extracted. For the data set shown here $P=-0.126\pm0.002$.

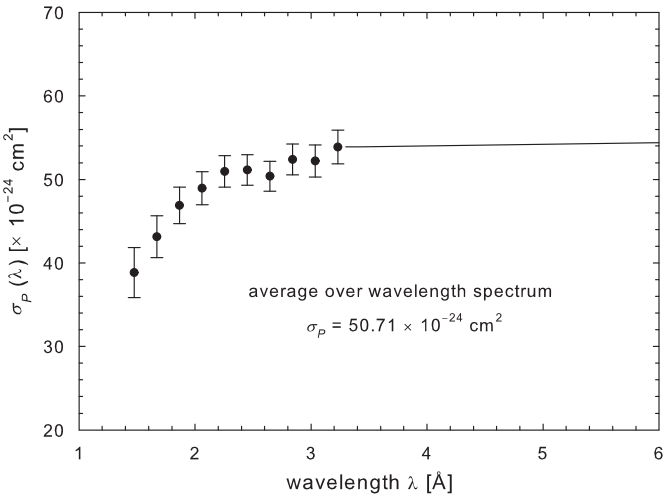

Fig. 10. Final polarization cross-section $\sigma_p(\lambda)$ where two data sets with comparable statistics have been combined. The line represents the value given by Eq. (6) which was combined with the experimental values (black dots) to determine the average over the wavelength spectrum.

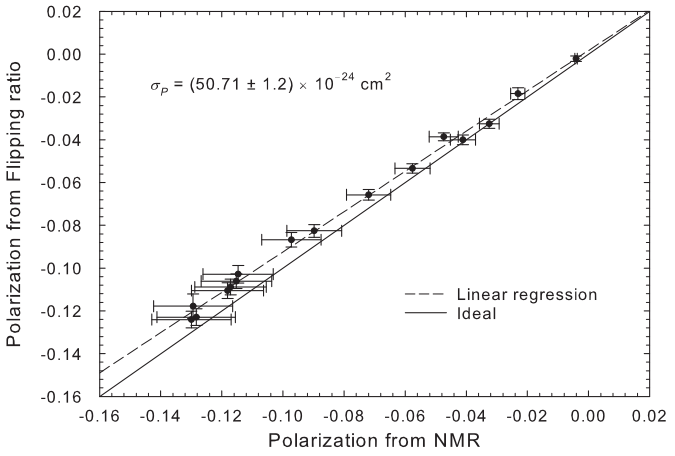

Fig. 11. Comparison between flipping ratio and NMR polarization determination. The error bars for the neutron measurement are mainly due to the cross-section and the beam polarization.

Fig. 8. It is seen that the analyzing power is about -0.17 at wavelengths above about 2.5 Å.

6.3. Determination of the polarization cross-section

Apart from demonstrating the analyzing power, our experiments also allow a precise determination of the proton spin polarization, independent of the NMR measurements. For this purpose we first use Eq. (2) to calculate the product

$$\sigma_p(\lambda)\cdot P=\frac{1}{Nd}\operatorname{artanh}(A(\lambda)) \tag{5}$$

from the analyzing power. Here we insert the target length $d=0.56\pm0.01$ cm and the proton density $N=4.285\times10^{22}$ cm^{-3} of naphthalene. The result is shown in Fig. 9.

To extract the proton spin polarization from the product $\sigma_p(\lambda)\cdot P$, we need to know the spin-dependent cross-section $\sigma_p(\lambda)$. At longer wavelengths, typically above several angstrom, the neutrons are scattered only incoherently out of the beam and $\sigma_p(\lambda)$ is independent of the host crystal of the proton spins. Then

$$\sigma_p(\lambda)=\sigma_{p,inc}+\sigma_{p,abs}\cdot\lambda \tag{6}$$

where $\sigma_{p,inc}=-(53.279\pm0.037)\times10^{-24}$ cm^2 is the part of the incoherent cross-section depending on the neutron spin orientation and $\sigma_{p,abs}=-(0.1849\pm0.0004)\times10^{-24}$ cm^2 Å^{-1} is the polarization dependent absorption [20].

In our case, where the spin filter is a single crystal with known unit cell, this lower limit for the validity of this equation can be calculated using Braggs law. Simulations performed with the software package FullProf [29] show that in our geometry – i.e. beam collimation and detector opening – coherent scattering can be safely excluded above 3 Å, even assuming a considerable disorientation of the crystal. We fit Eq. (6) to the experimental values of the product $\sigma_p(\lambda)\cdot P$ in the range 3.3–9.5 Å and thus extract the proton polarization P. For the data shown in Fig. 9 the result is $P=-0.126\pm0.002$.

Using the thus obtained value of the proton spin polarization P we obtain the polarization cross-section $\sigma_p(\lambda)$ below 3.3 Å using Eq. (5). The combined results for $\sigma_p(\lambda)$ for two TOF spectra are shown as

black dots in Fig. 10. The drawn line represents Eq. (6). Finally, the wavelength averaged polarization cross-section is determined using the experimental values of $\sigma_p(\lambda)$ below $\lambda = 3.3$ Å (the black dots in Fig. 10) and Eq. (6) above $\lambda = 3.3$ Å (the drawn line in Fig. 10). The result is $\overline{\sigma}_p = (50.71 \pm 1.2) \times 10^{-24}$ cm^2.

6.4. Neutrons as polarization probe

Now the averaged polarization cross-section $\overline{\sigma}_p$ is determined, the proton polarization P of the sample can be determined rapidly by measuring the flipping ratio R_F with the white beam using the average $\overline{p}$ of the beam polarization presented in Fig. 7

$$P = \frac{1}{\overline{\sigma}_p}\frac{1}{Nd}\operatorname{artanh}\left(\frac{R_F - 1}{R_F f + 1}\frac{1}{\overline{p}}\right). \quad (7)$$

We compared the thus obtained polarization with the polarization determined by NMR for different polarization levels. As is seen in Fig. 11 the results are found to be in good agreement.

7. Probing the optical excitation process

Diminishing the laser power reduces the number of triplet states as can be directly observed as a smaller ESR signal. Also the polarization is seen to grow more slowly and reach a lower final level. An important question is however how far a laser pulse containing considerably less photons than pentacene molecules penetrates into the sample. Model calculations suggest a strong gradient in the number of the triplet states that are created along the beam path [30]. This would result in a strong gradient in the proton polarization along this path.

With the method described above we are able to measure the proton polarization as a function of the position in the sample using a tiny neutron beam. We scan the sample with a beam which is collimated to a hight of slightly less than 1 mm and measure the flipping ratio at different vertical positions of the sample, i.e., at different positions along laser path (see Fig. 4). Such scans have been performed after having reached a saturated polarization level for three different laser pulse energies of 9.6, 2.1 and 1.0 mJ, respectively, measured at the entrance window of the cryostat. The results for the proton spin polarization as a function of the position in the sample are shown in Fig. 12. It is seen that in all cases the polarization is homogeneous over the sample along the laser beam direction. The strong slopes on the sides start to appear when part of the neutron beam passes above or below the sample and is thus not spin analyzed. As spin diffusion is too slow to homogenize the sample polarization, we conclude that the triplet states have been created homogeneously over the sample. Observe that a laser pulse of 1.0 mJ at 602 nm contains 0.33×10^{16} photons which is much lower than the number $n_p = 1.5 \times 10^{16}$ of pentacene molecules in the sample. We conclude that predicted strong gradients are not observed in our sample.

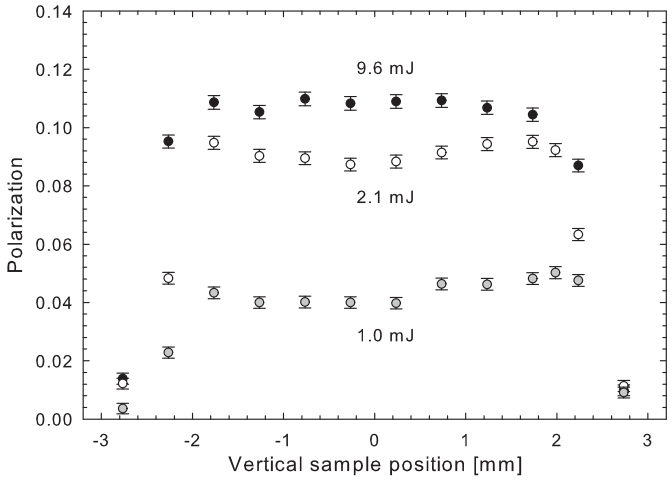

Fig. 12. Polarization homogeneity in the sample for different powers of laser excitation. The data points were obtained by measuring the neutron flipping ratio of the white beam collimated to less than 1 mm. The errors are due to the statistic uncertainty of the flipping ratio.

8. Conclusion

We believe that we have provided a proof of principle of a neutron spin filter consisting of a single crystal of naphthalene in which the proton spins are polarized using DNP with photo-excited triplet states. Our apparatus can be operated reliably over periods of several weeks. The analyzing power obtained thus far – $A = 0.17$ – is still modest, due to the still small maximum proton spin polarization – $P \sim 0.13$. It is expected that a more adequate laser system allows the polarization to increase by a factor of the order three [25] and – using our present system – the analyzing power could attain values of around 0.45. Increasing the thickness of the sample to 10 mm increases the analyzing power even further than 0.7. Another limitation of our present setup is the small size of the polarized target. We are investigating the possibility to reduce the beam diameter with focusing guides [31].

The neutron beam was also used to analyze the polarized target employed in the spin filter. We obtained an independent measurement of the proton spin polarization which is in good agreement with the value determined with NMR. Moreover, the neutron beam was used to measure the proton spin polarization as a function of position in the naphthalene sample. The polarization was found to be homogeneous, even at low laser power. This is in contradiction to existing models describing the photo-excitation process [30]. Further study is needed to explain the results.

Acknowledgments

We especially acknowledge the technical support by P. Schurter, whose outstanding skills have made these experiments possible. We are further indebted to J.J. van der Klink, A. Comment and S. Jannin for the design of the ESR/DNP spectrometer and U. Filges and T. Panzner for assistance in commissioning the BOA beam line. This work was supported by the Swiss National Science Foundation grant 200020_124901.

References

[1] A. Abragam, M. Goldman, Reports on Progress in Physics 41 (1978) 395.
[2] J.B. Hayter, G.T. Jenkin, J.W. White, Physical Review Letters 33 (1974) 696.
[3] H.B. Stuhrmann, Reports on Progress in Physics 67 (2004) 1073.
[4] B. van den Brandt, H. Glättli, I. Grillo, P. Hautle, H. Jouve, J. Kohlbrecher, J.A. Konter, E. Leymarie, S. Mango, R.P. May, A. Michels, H.B. Stuhrmann, O. Zimmer, European Physical Journal B 49 (2006) 157.
[5] A. Henstra, T.-S. Lin, J. Schmidt, W.Th. Wenckebach, Chemical Physics Letters 165 (1990) 6.
[6] O. Schaerpf, Physica B 156 & 157 (1989) 639.
[7] V.I. Lushchikov, Yu.V. Taran, F.L. Shapiro, Soviet Journal of Nuclear Physics 10 (1970) 669.
[8] R. Surkau, J. Becker, M. Ebert, T. Grossmann, W. Heil, D. Hofmann, H. Humblot, M. Leduc, E.W. Otten, D. Rohe, K. Siemensmeyer, M. Steiner, F. Tasset, N. Trautmann, Nuclear Instruments and Methods in Physics Research Section A 384 (1997) 444.
[9] O. Zimmer, T.M. Müller, P. Hautle, W. Heil, H. Humblot, Physics Letters B 455 (1999) 62.

[10] O. Zimmer, P. Hautle, W. Heil, D. Hofmann, H. Humblot, I. Krasnoschekova, M. Lasakov, T.M. Müller, V. Nesvizhevsky, J. Reich, A. Serebrov, Yu. Sobolev, A. Vassilev, Nuclear Instruments and Methods in Physics Research Section A 440 (2000) 764.
[11] I. Anderson, J. Cook, G. Felcher, T. Gentile, G. Greene, F. Klose, T. Koetzle, E. Lelièvre-Berna, A. Parizzi, R. Pynn, J. Zhao, Journal of Neutron Research 13 (2005) 193.
[12] ⟨http://jra4.neutron-eu.net/jra4/⟩.
[13] A. Schebetov, A. Serebrov, V.M. Pusenkov, M. Lasakov, P. Böni, M. Lüthy, J. Sromicki, Nuclear Instruments and Methods in Physics Research Section A 497 (2003) 479.
[14] V.K. Aswal, B. van den Brandt, P. Hautle, J. Kohlbrecher, J.A. Konter, A. Michels, F.M. Piegsa, J. Stahn, S. Van Petegem, O. Zimmer, Nuclear Instruments and Methods in Physics Research Section A 586 (2008) 86.
[15] S. Hiramatsu, S. Isagawa, S. Ishimoto, A. Masaike, K. Morimoto, S. Funahashi, Y. Hamaguchi, N. Minakawa, Y. Yamaguchi, Journal of the Physical Society of Japan 45 (1978) 949.
[16] P.P.J. Delheij, J.D. Bowman, C.M. Frankle, D.G. Haase, T. Langston, R. Mortensen, S. Penttila, H. Postma, S.J. Seestrom, Y.-F. Yen, Nuclear Instruments and Methods in Physics Research Section A 356 (1995) 120.
[17] M. Iinuma, Y. Takahashi, I. Shaké, M. Oda, A. Masaike, T. Yabuzaki, H.M. Shimizu, Nuclear Instruments and Methods in Physics Research Section A 529 (2004) 199.
[18] A. Abragam, M. Goldman, Nuclear Magnetism: Order and Disorder, Oxford University Press, 1982.
[19] H. Glättli, M. Goldman, in: Methods of Experimental Physics, Part C, vol. 23, Academic Press, New York, 1987, pp. 241–286.
[20] A.-J. Dianoux, G. Lander (Eds.), ILL Neutron Data Booklet, OCP Science Imprint, Philadelphia, 2003.
[21] V.F. Turchin, Slow Neutrons, Israel Program for Scientific Translations, Jerusalem, 1965.
[22] P. Hautle, W. Heil, D. Hofmann, H. Humblot, T.M. Müller, O. Zimmer, in: Proceedings of the 9th International Workshop on Polarised Sources and Targets, Nashville 2001, World Scientific, Singapore, 2002, p. 274.
[23] A.J. van Strien, J. Schmidt, Chemical Physics Letters 70 (1980) 513.
[24] A. Henstra, P. Dirksen, W.Th. Wenckebach, Physics Letters A 134 (1988) 134.
[25] M. Iinuma, Y. Takahashi, I. Shaké, M. Oda, A. Masaike, T. Yabuzaki, Physical Review Letters 84 (2000) 171.
[26] T. Uesaka, T. Wakui, S. Sakaguchi, T. Kawahara, H. Sakai, European Physical Journal Special Topics 150 (2007) 71.
[27] S. Selvakumar, K. Sivaji, A. Arulchakkaravarthi, N. Balamurugan, S. Sankar, P. Ramasam, Journal of Crystal Growth 282 (2005) 370.
[28] O. Zimmer, Physics Letters B 461 (1999) 307.
[29] ⟨http://www.ill.eu/sites/fullprof/⟩.
[30] K. Takeda, K. Takegoshi, T. Terao, Journal of Chemical Physics 17 (2002) 4940.
[31] P. Böni, Nuclear Instruments and Methods in Physics Research Section A 586 (2008) 1.